Histol Histopathol (2002) 17: 1-7
DOI: 10.14670/HH-17.1

http://www.hh.um.es

Histology and Histopathology
Cellular and Molecular Biology

Sex- and strain-dependent histological features of the proximal convoluted tubular epithelium of mouse kidney: association with lysosomes containing apolipoprotein B

A. Yabuki[1], S. Suzuki[2], M. Matsumoto[1] and H. Nishinakagawa[1]

[1]Department of Veterinary Anatomy, Faculty of Agriculture, Kagoshima University, Kagoshima, Japan and
[2]Institute of Laboratory Animal Sciences, Faculty of Medicine, Kagoshima University, Kagoshima, Japan

Summary. In the present study, we performed comparative histological observations of ICR, BALB/c, C57BL/6, C3H/HeN and DBA/2 mice kidneys. Sex and strain differences were observed in the appearance of vacuolar structures of the proximal convoluted tubules (toluidine blue-positive granules in osmium-postfixed epoxy-resin sections). These features were especially remarkable in male DBA/2 mice. The vacuolar structures in male DBA/2 mice showed heterogeneous staining with Sudan B in frozen sections and appeared under an electron microscope as multilammelar giant dense bodies. In addition, these dense bodies showed heterogeneous acid phosphatase reactions. Immunohistochemical analyses of these structures for apolipoprotein B showed strong positive reactions. These results suggested that vacuolar structures in the proximal convoluted tubules, which were remarkable in male DBA/2 mice, were giant lysosomes containing apolipoprotein B.

Key words: Kidney, Lysosome, Mouse, Sex, Strain

Introduction

Renal structural alterations are closely related to their functional alterations, and renal histopathological analysis is indispensable to investigations of renal failure. To correct interpretation of histopathological observations in laboratory experiments, an understanding of normal histological features of laboratory animals is very important.

The mouse has been used frequently in laboratory experiments, and there have been many reports regarding sexual dimorphism of the mouse kidneys. For example, the parietal layers of renal corpuscles in males are comprised of a cuboidal epithelium, whereas those in females consist of a squamous epithelium (Messow et al., 1980; Ahmadizadeh et al., 1984; Barberini et al., 1984; Yabuki et al., 1999b). The cytological figures of mitochondria and lysosomes in the proximal tubules were different between males and females (Koenig et al., 1980). In the proximal straight tubules (PST), heavy periodic acid Schiff (PAS) staining of the brush border and abundant PAS-positive granules have been observed in females (Yabuki et al., 1999a). In addition, these features in the PST have been shown to differ depending on strain (Yabuki et al., 2001). However, sex- and strain-dependent structural features have not been fully clarified, except for the previously described studies.

In the present study, we performed comparative observations about mouse renal structures by the use of five mouse strains, and found the sex- and strain-dependent differences of vacuolar structures in the proximal convoluted tubules (PCT). Furthermore, we performed cytological, cytochemical and immunohistochemical observations to examine the functional role of such vacuolar structures.

Offprint requests to: Akira Yabuki, Department of Veterinary Anatomy, Faculty of Agriculture, Kagoshima University, 21-24 Korimoto 1, Kagoshima-shi, Kagoshima 890-0065, Japan. Fax: +81-99-285-8710. e-mail: yabu@vet.agri.kagoshima-u.ac.jp

Materials and methods

All experiments were carried out in accordance with the Guideline for Animal Experimentation of the Faculty of Agriculture, Kagoshima University, Japan.

Environment of animal housing

All mice used in the present study were housed in an open system room with a one-way airflow system (temperature; 22±1 °C, humidity; 55±10%, light period; 07:00 h-19:00 h, ventilation; 12 times/hr) in the Institute of Laboratory Animal Sciences, Faculty of Medicine, Kagoshima University, Japan. The mice received an autoclaved commercial diet (CE-2, Japan CLEA., JAPAN) and tap water *ad libitum*.

Light microscopy (LM) and transmission electron microscopy (TEM)

Eight female and eight male three- to four-month-old mice from each strain (Jcl: ICR, BALB/cA Jcl (BALB/c), C57BL/6J Slc (C57BL/6), C3H/HeN Jcl (C3H/HeN) and DBA/2Cr Slc (DBA/2)) were used in the investigation. All animals were dissected by exsanguination under anesthesia (a mixture of ketamine and medetomidine) and their kidneys were quickly removed. From the left kidneys, central slices that included the hilum were cut perpendicular to the long axis and fixed in 10% neutral-buffered formalin at room temperature (RT). The slices were then routinely embedded in paraffin. Sections, 3 µm in thickness, were stained with hematoxylin-eosin (HE), PAS, and toluidine blue (TB). From the right kidneys, small pieces, approximately 1 mm thick, were cut from the cortex and fixed in a mixture of 2.5% glutaraldehyde and 2% paraformaldehyde in 0.1M phosphate buffer (PB, pH 7.4) for 2 hrs at 4 °C. After washing in cold PB, the specimens were postfixed in 1% osmium tetroxide in PB for 2 hrs at 4 °C. The specimens were then dehydrated through a graded ethanol series and embedded in epoxy-resin. Sections, 1 µm thick, were cut from separate epoxy-resin blocks (five sections per animal), mounted on glass slides, and stained with TB without prior removal of the epoxy-resin. To objectively estimate the appearance of TB-positive granules in the PCT, each epoxy-resin section was scored from 0 to 5 at random under LM, as follows: 0, no or few small granules in the PCT epithelium; 1, small granules frequently observed in the PCT epithelium; 2, many small granules observed in the PCT; 3, in addition to many small granules, giant granules, larger than the size of the nuclei, observed sporadically in the PCT epithelium; 4, in addition to many small granules, giant granules frequently observed in the PCT epithelium; and 5, in addition to many small granules, many giant granules observed in the PCT epithelium. From the mean score of each animal, we ranked the appearance of TB-positive granules in the PCT, as follows: - (mean≤0.5), +1 (0.5<mean≤ 1.5), +2 (1.5<mean≤ 2.5), +3 (2.5<mean≤ 3.5), +4 (3.5<mean≤ 4.5), and +5 (4.5<mean). Ultrathin sections were stained with uranyl acetate and lead citrate, and observed by TEM (H-7000KU, Hitachi, Japan).

Three-month-old male DBA/2 mice (n=3) were used in the remaining investigations. The animals were perfused through the left ventricle with cold physiological saline for 30 sec and then with a cold mixture of 1.25% glutaraldehyde and 2% paraformaldehyde in PB for 10 min under anesthesia, and the right and left kidneys were removed. From the left kidneys, central slices were cut perpendicular to the long axis and immersed overnight in a mixture of 2.5% glutaraldehyde and 2% paraformaldehyde in PB at 4 °C. After washing in PB, tissue slices were divided into two pieces. One piece was routinely embedded in paraffin and 3 µm-thick sections were stained with HE, PAS, and TB. The second piece was embedded in gelatin prior to preparation of frozen sections. Frozen sections were cut by a microtome equipped with a thermo-electric freezing unit (Komatsu Electronics, Japan) and stained with Sudan B. From the right kidneys, small cortical pieces were cut and fixed in a mixture of 2.5% glutaraldehyde and 2% paraformaldehyde in PB for 2 hrs at 4 °C. After washing in cold PB, the pieces were postfixed in osmium tetroxide in PB and embedded in epoxy-resin, as described above.

Immunohistochemical detection of apolipoprotein B

Several cortical pieces from the right kidneys of the male DBA/2 mice, which were fixed by perfusion, were thoroughly washed in cold PB without further fixation. Sections, 200 µm thick, were cut by a microslicer (DTK-1000, Dosaka EM, JAPAN) and postfixed in a low potassium ferrocyanide-reduced osmium (Neiss, 1984) for 45 min at 4 °C. After washing in PB, the samples were serially dehydrated, embedded in LR white resin, and polymerized at 50 °C for 48 hrs. Sections, 2 µm thick, were cut and mounted on the mesh cement-coated glass slides. After immersion in 0.1M Tris-buffered saline (TBS, pH 7.4), the sections were blocked with 1% bovine serum albumin in TBS and incubated overnight with rabbit polyclonal anti-human apolipoprotein B (Calbiochem, USA) diluted 1:100 in TBS at 4 °C. After washing in TBS, the samples were incubated for 2 hrs at RT with alkaline phosphatase-conjugated goat anti-rabbit IgG (Vector Laboratories, USA) diluted 1:100 in TBS, and washed again in TBS. Immunoreactivity was visualized as a red color by an alkaline phosphatase substrate kit (Vector Red, Vector Laboratories, USA) and counterstained with hematoxylin. To block the endogenous alkaline phosphatase, 1 mM of levamisole was added to the substrate solution. Negative control sections were incubated with TBS instead of primary antibody.

Acid phosphatase (AcPase) reaction

Three-month-old male DBA/2 mice (n=3) were used for detection of AcPase reaction by TEM. The mice were perfused under anesthesia with a cold mixture of 2.0% glutaraldehyde and 2% paraformaldehyde in 0.1M cacodylate buffer (CB, pH 7.4) for 10 min, followed by perfusion with cold physiological saline. After perfusion, small cortical pieces of the left kidneys were thoroughly washed in CB containing 5% saccharose and 40 µm-thick sections were cut by a microslicer. The sections were incubated with Gomori's AcPase reaction solution (Gomori, 1952), using ß-glycerophosphate as the substrate, for 30 min at 37 °C. Negative control sections were incubated with the solution to remove the substrate. After washing in CB containing 5% saccharose, the sections were postfixed in 1% osmium tetroxide in CB for 1 hr at 4 °C and routinely embedded in epoxy-resin. Ultrathin sections were not stained prior to TEM

observations.

Results

Histological observations

In paraffin sections, sex- or strain-based structural features in the glomerular capsules and PST epithelium were confirmed. The parietal layers of the glomerular capsules in males consisted of a cuboidal epithelium (Fig. 1). In the PST epithelium, PAS staining of the brush borders in females was stronger than that in males, and this staining difference was remarkable in ICR strain (Fig. 2). The PAS-positive granules were observed in the PST epithelium of females, especially remarkable in female DBA/2 mice (Fig. 3).

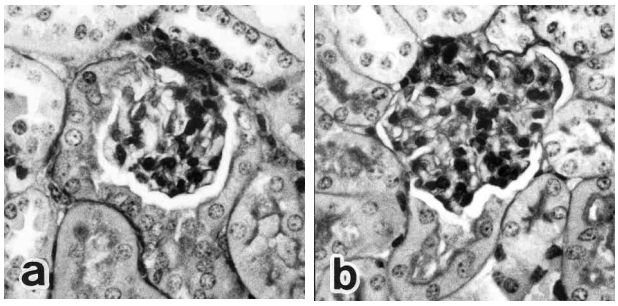

Fig. 1. Light micrographs of the renal corpuscles in the C3H/HeN mice kidneys. **a.** Male mice. The parietal layer of the glomerular capsule consists of a cuboidal epithelium. **b.** Female mice. The parietal layer of the glomerular capsule consists of a squamous epithelium. PAS. x 350

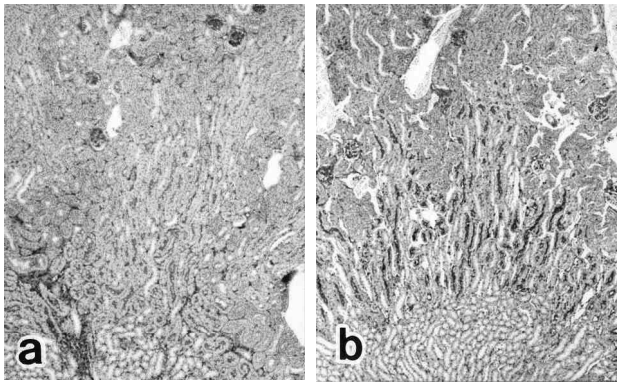

Fig. 2. Light micrographs of the ICR mice kidneys. **a.** Male mice. **b.** Female mice. The staining intensity of the brush borders of PST in the outer medulla is stronger in females **(b)** than that in males **(a)**. PAS. x 35

Fig. 3. Light micrographs of the outer medulla. **a.** Male C57BL/6 mice. No granules are seen in the PST epithelium. **b.** Female C57BL/6 mice. A small number of granules (small arrows) are seen in the PST epithelium. **c.** Female DBA/2 mice. In addition to many small granules, giant granules (large arrows), larger than the size of the nuclei, are observed in the PST epithelium. PAS. x 350

Except for the features described above, in the PCT epithelium on the paraffin sections, vacuolar structures, which did not stain with HE, PAS or TB stains, were particularly remarkable in male DBA/2 mice (Fig. 4c). Such vacuolar structures were not observed in the initial portions of PCT (Fig. 4c). In epoxy-resin sections, these vacuolar structures were observed as TB-positive granules (Fig. 4d). Although vacuolar structures were unclear except for male DBA/2 mice (Fig. 4a, c and e), TB-positive granules in the PCT epithelium were also observed in males of other strains or in females of all strains (Fig. 4b,f). Table 1 shows the results of semiquantitative analysis about TB-positive granules of the PCT epithelium. In ICR, BALB/c, C3H/HeN, and DBA/2 mice, the males were ranked higher than the females. In contrast, in C57BL/6 mice, the males were ranked lower than the females. Among all strains of both sexes, male DBA/2 mouse exhibited the most pronounced granules and all of male DBA/2 were ranked as +5 grade. The vacuolar structures or TB-positive granules in the PCT of male DBA/2 mice were also observed by use of a perfusion-fixation technique, therefore possibility of artifacts was denied. In Sudan B stain, these structures showed heterogeneous staining (strongly positive, slightly positive, or negative) (Fig. 5).

Cytological, cytochemical, and immunohistochemical observations

Further investigations were performed to focus on the vacuolar structures (TB-positive granules in) of the PCT epithelium. In TEM observation, electron-dense

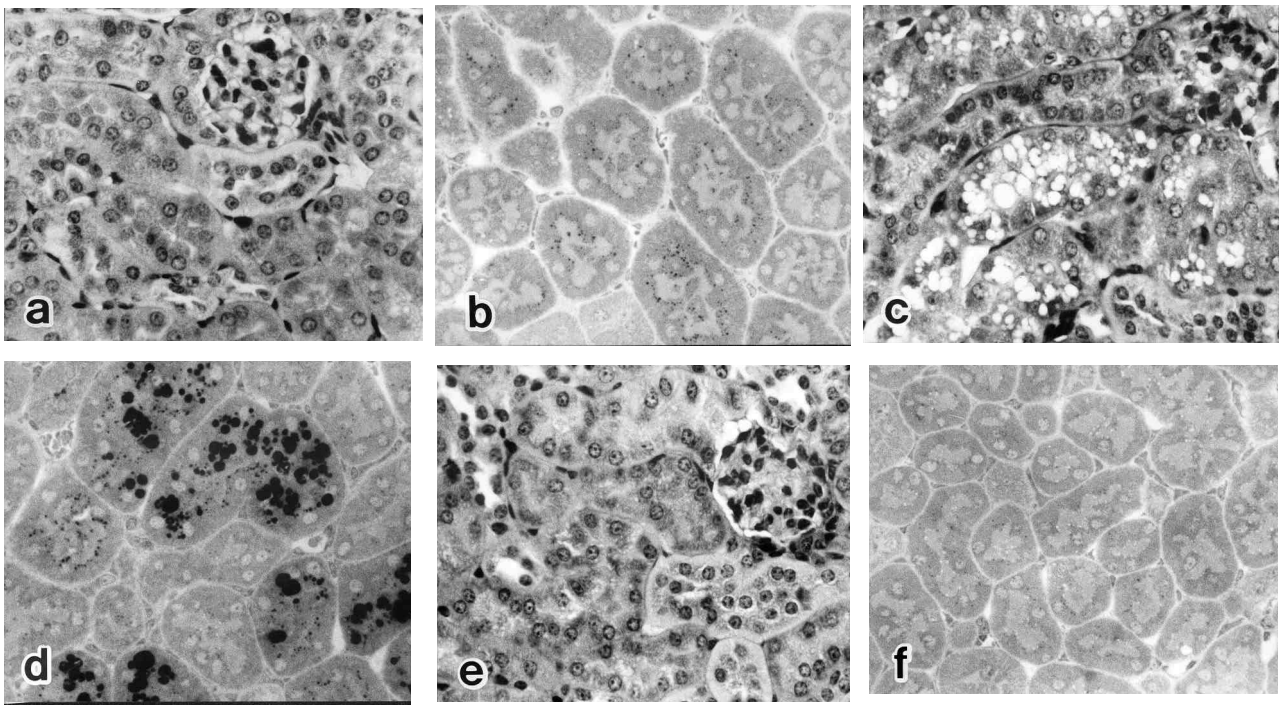

Fig. 4. Light micrographs of mouse kidneys. **a, c and e.** Paraffin sections stained with TB. **b, d and f.** Epoxy-resin sections stained with TB. **a and b.** Male C3H/HeN mice. **c and d.** Male DBA/2 mice. **e and f.** Female DBA/2 mice. Vacuolar structures **(c)** and TB-positive granules **(d)** are apparent in the PCT epithelium of male DBA/2 mice. x 300

Table 1. Rank of the animals which on the number and size of TB-positive granules in the PCT epithelium.

STRAIN	ICR		BALB/c		C3H/HeN		C57BL/6		DBA/2	
SEX	M	F	M	F	M	F	M	F	M	F
-[1)]	0 [2)]	8	0	0	0	0	0	0	0	6
+1	2	0	0	7	1	5	7	3	0	2
+2	3	0	2	1	6	3	1	5	0	0
+3	2	0	4	0	1	0	0	0	0	0
+4	1	0	2	0	0	0	0	0	0	0
+5	0	0	0	0	0	0	0	0	8	0

M: males. F: females. [1)]: -, mean≤ 0.5; +1, 0.5<mean≤ 1.5; +2, 1.5<mean≤ 2.5; +3, 2.5<mean≤ 3.5; +4, 3.5<mean≤ 4.5, +5, 4.5<mean≤ 5.0. [2)]: each value represents the number of animal.

bodies were apparent in male DBA/2 mice, and these dense bodies were considered as the vacuolar structures in the paraffin sections (Fig. 6). These bodies consisted of high electron- and slightly high electron-dense matrices, and their size varied and giant bodies were often larger than the nucleus. Fuse figures were frequently observed, and these bodies contained multilamellar structures.

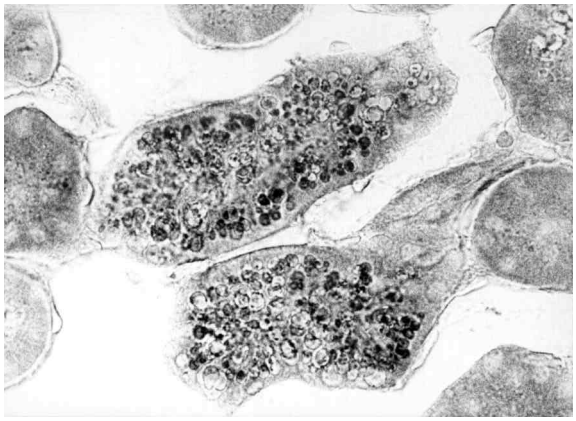

Fig. 5. Light micrograph of a renal frozen section from a male DBA/2 mouse. The section is stained with Sudan B. Cytoplasmic granules of PCT show heterogeneous staining, i.e. strongly positive, slightly positive or negative. x 400

AcPase activity was strongly observed in small bodies (Fig. 7a), whereas large bodies showed weak activity that was localized in the marginal areas (Fig. 7b). Positive reactions were often detected in the fusion areas (Fig. 7d). Most giant bodies were negative for AcPase activity (Fig. 7c). Electron-dense central matrices of large and giant bodies were considered as negative reactions (Fig. 7e).

In the immunohistochemical observation, cytoplasmic granules in the PCT epithelium were red in color and thus strongly positive for apolipoprotein B (Fig. 8a). In negative control sections, cytoplasmic granules of PCT appeared black due to the tissue preparation procedures (Fig. 8b).

Discussion

In the present comparative histological investigation in the kidneys of ICR, BALB/c, C57BL/6, C3H/HeN,

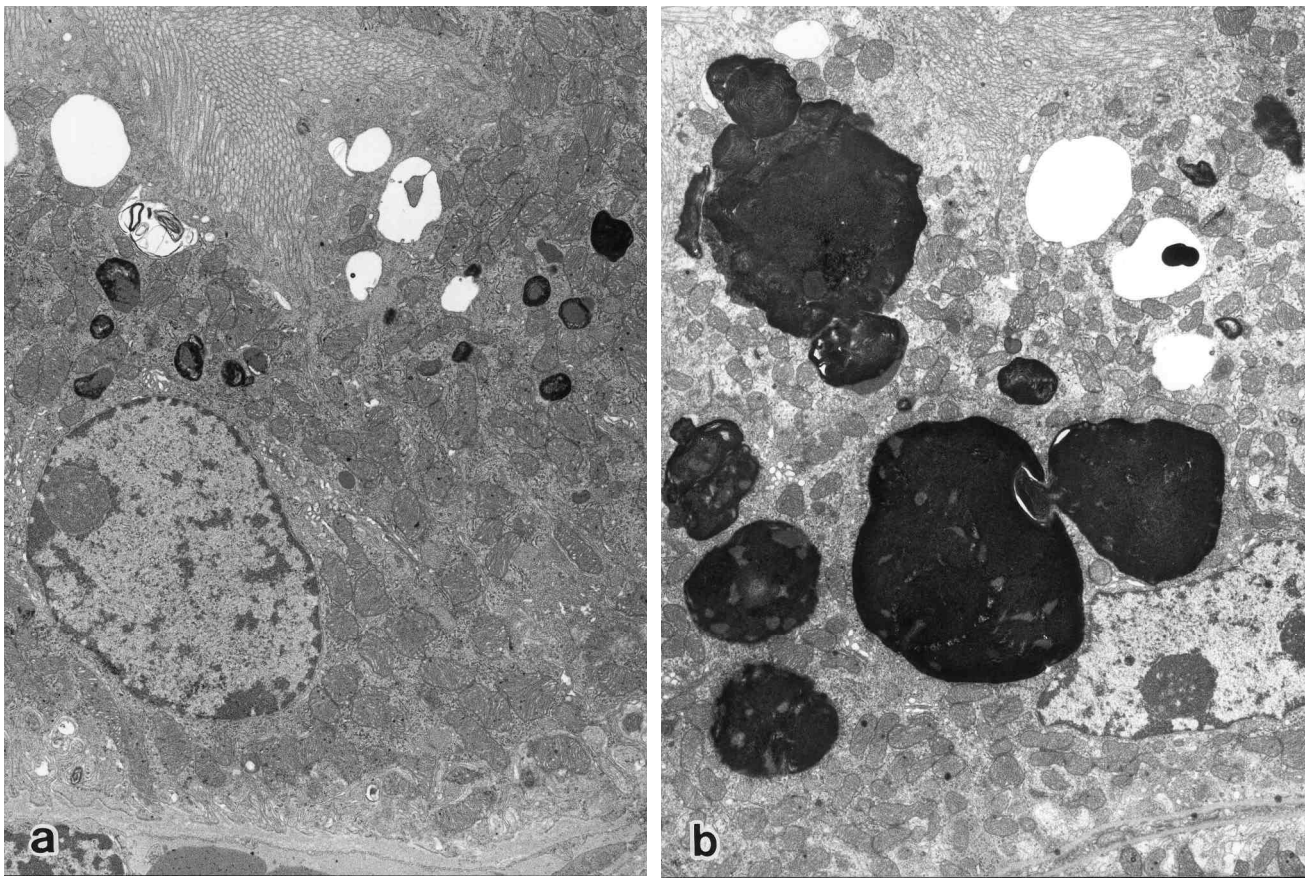

Fig. 6. Electron micrograph of the PCT cells in male mice kidneys. **a.** C3H/HeN mice. The size of the electron-bodies is similar to those of the mitochondria. **b.** DBA/2 mice. The size of the electron-dense bodies is apparently larger than that of the C3H/HeN mice **(a)**, and fusion figures of these bodies are frequently observed. x 6,250

and DBA/2 mice, we confirmed the previously reported mouse renal structural features (Messow et al., 1980; Ahmadizadeh et al., 1984; Barberini et al., 1984; Yabuki et al., 1999a,b, 2001). Moreover, we detected sex- and strain-dependent differences of vacuolar structures (TB-positive granules) in the PCT epithelium. These vacuolar structures were especially remarkable in male DBA/2 mice. From the findings of the heterogeneous staining with Sudan B, the ultrastructural features and the heterogeneous AcPase reactions, we suggested that these vacuolar structures were not simple lipid droplets but lysosomes, which contain various amounts of lipids. The size of these lysosomes increased due to fusion, although as these lysosomes became larger, their AcPase activities weakened.

Recent reports indicate that the renal proximal tubule plays an important role in the catabolism of low-density lipoprotein (LDL)., e.g. LDL receptor family is distributed throughout the renal proximal tubules (Christensen et al., 1995, 1998; Stefansson et al., 1995;

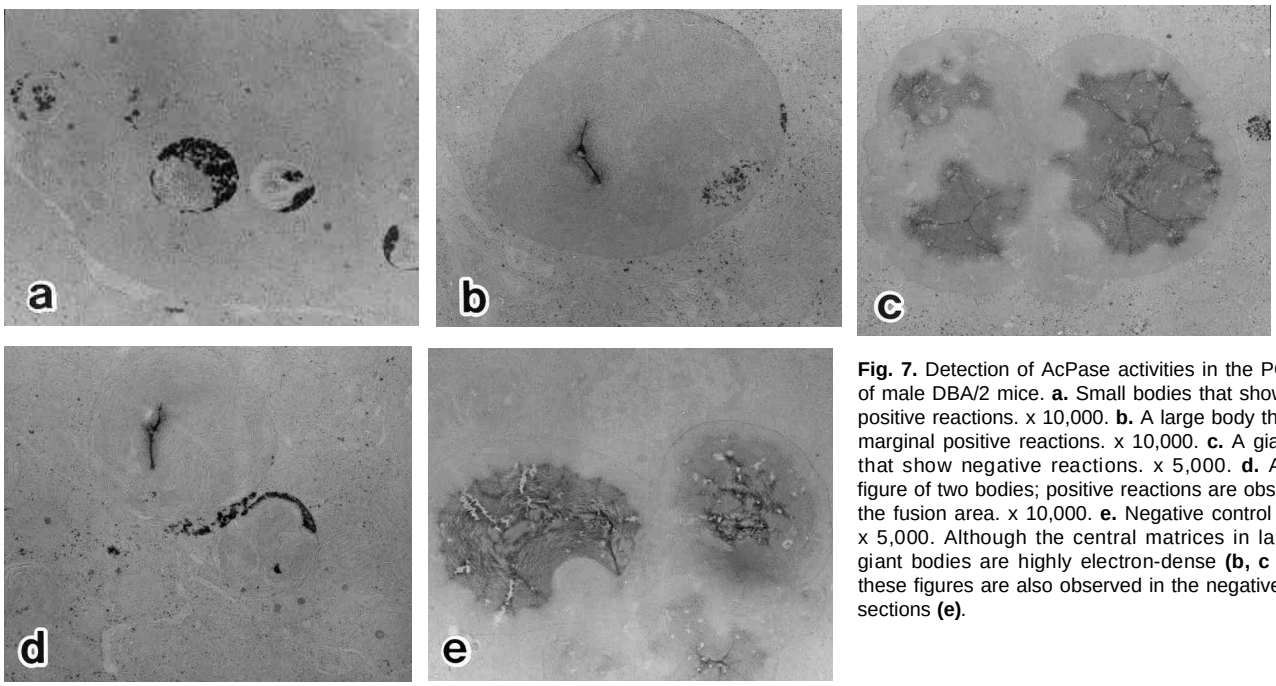

Fig. 7. Detection of AcPase activities in the PCT cells of male DBA/2 mice. **a.** Small bodies that show strong positive reactions. x 10,000. **b.** A large body that show marginal positive reactions. x 10,000. **c.** A giant body that show negative reactions. x 5,000. **d.** A fusion figure of two bodies; positive reactions are observed in the fusion area. x 10,000. **e.** Negative control section. x 5,000. Although the central matrices in large and giant bodies are highly electron-dense **(b, c and d)**, these figures are also observed in the negative control sections **(e)**.

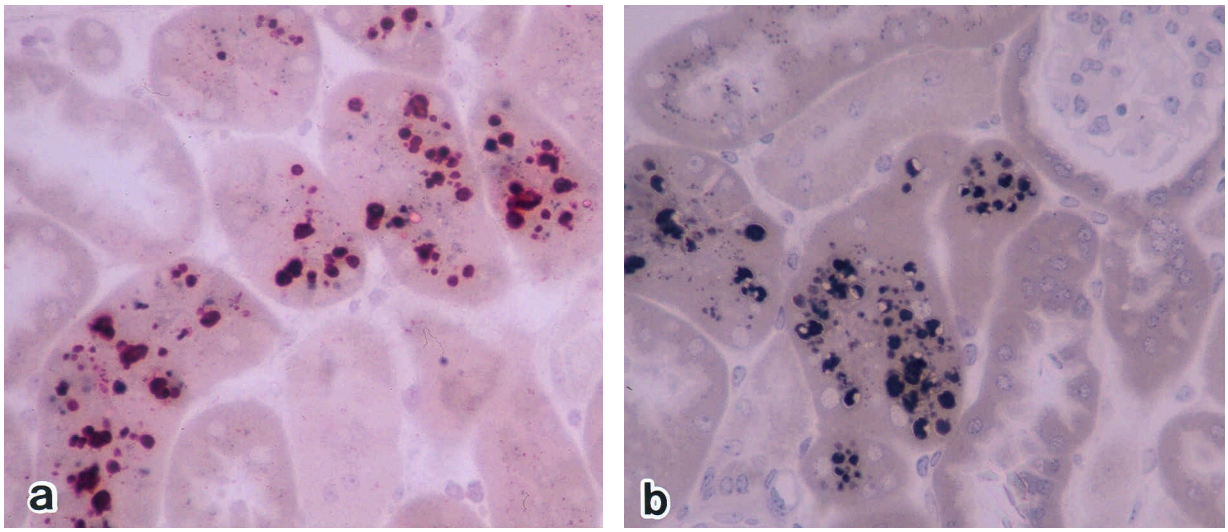

Fig. 8. Detection of apolipoprotein B in the kidneys of male DBA/2 mice. **a.** Cytoplasmic granules of the PCT epithelium show strong positive reactions, which manifest as a red color. **b.** Negative control section; granules of the PCT epithelium appear black in color. x 400

Chen et al., 1999; Birn et al., 2000), and autoradiographic analysis has demonstrated the active uptake of LDL in the proximal tubules (Chen et al, 1999). Therefore, we propose that a main function of the lysosomal granules in the present study is related to LDL metabolism. To test this conjecture, we used immunohistochemistry to detect apolipoprotein B, which is a component protein of LDL. Granules in the PCT were strongly positive for apolipoprotein B, which supports the proposed role of the cytoplasmic granules in LDL metabolism.

Renal structures resembling vacuolar structures of male DBA/2 mice were previously reported in cat (Bargmann et al., 1977) and mastomys kidneys (Fujimura et al., 1996). However, these structures of cat were characterized by TEM as electron-lucent bodies, which were not surrounded by a membrane, and those of mastomys showed negative staining for lipids in frozen sections. We recently reported PAS-positive giant granules in the PST epithelium of female DBA/2 mice (Yabuki et al., 2001). The staining characteristics of these granules differ from those of the vacuolar structures of PCT in male DBA/2 mice. However, their sizes, ultrastructural features and AcPase reactions of the female PST granules resembled male PCT vacuolar structures. Since these observations were made in the same mouse strain, we believe that these granules and vacuolar structures may be closely related. Although sexual dimorphism of the lysosomal size (larger in males) in the proximal tubules has been demonstrated in the A/J mouse strain (Koenig at al., 1980), such giant lysosomes as detected in the male PCT or female PST cells of the DBA/2 strain have not been known in the kidneys of common mouse strains. Further investigations are necessary to clarify the functional roles of these giant lysosomes.

References

Ahmadizadeh M., Echt R., Kuo C.H. and Hook J.B. (1984). Sex and strain differences in mouse kidney: Bowman's capsule morphology and susceptibility to chloroform. Toxicol. Lett. 20, 161-172.

Barberini F., Familiari G., Vittori I., Carpino F. and Melis M. (1984). Morphological and statistical investigation of the occurrence of 'Tubule-like cells' in the renal corpuscle of the mouse kidney induced by sex hormones. Renal. Physiol. 7, 227-236.

Bargmann W., Krisch B. and Leonhardt H. (1977). Lipids in the proximal convoluted tubule of the cat kidney and reabsorption of cholesterol. Cell Tissue Res. 177, 523-538.

Birn H., Vorum H., Verroust P.J., Moestrup S.K. and Christensen E.I. (2000). Receptor-associated protein is important for normal processing of megalin in kidney proximal tubules. J. Am. Soc. Nephrol. 11, 191-202.

Chen Z., Saffitz J.E., Latour M.A. and Schonfeld G. (1999). Truncated apo B-70.5-containing lipoproteins bind to megalin but the LDL receptor. J. Clin. Invest. 103, 1419-1430.

Christensen E.I., Nielsen S., Moestrup S.K., Borre C., Maunsbach A.B., de Heer E., Ronco P., Hammond T.G. and Verroust P. (1995). Segmental distribution of the endocytosis receptor gp330 in renal proximal tubules. Eur. J. Cell Biol. 66, 349-364.

Christensen E.I., Birn H., Verroust P. and Moestrup S.K. (1998). Megalin-mediated endocytosis in renal proximal tubule. Ren. Fail. 20, 191-199.

Fujimura H., Ogura A., Asano T., Noguchi Y., Mochida K. and Takimoto K. (1996). Lysosomal glycolipid storage in the renal tubular epithelium in mastomys (*Praomys coucha*). Histol. Histopathol. 11, 171-174.

Gomori G. (1952). Microscopic histochemistry. The University of Chicago Press. Chicago. 3, 193.

Koenig H., Goldstone A., Blume G. and Lu C.Y. (1980). Testosterone-mediated sexual dimorphism of mitochondria and lysosomes in mouse kidney proximal tubules. Science 209, 1023-1026.

Messow C., Gärtner K., Hackbarth H., Kangaloo M. and Lünebrink L. (1980). Sex differences in kidney morphology and glomerular filtration rate in mice. Contr. Nephrol. 19, 51-55.

Neiss W.F. (1984). Electron staining of the cell surface coat by osmium-low ferrocyanide. Histochemistry 80, 231-242.

Stefansson S., Chappell D.A., Argraves K.M., Strickland D.K, and Argraves W.S. (1995). Glycoprotein 330/low density lipoprotein receptor-related protein-2 mediates endocytosis of low density lipoprotein via interaction with apolipoprotein B100. J. Biol. Chem. 270, 19417-19421.

Yabuki A,. Suzuki S., Matsumoto M. and Nishinakagawa H. (1999a). Sexual dimorphism of proximal straight tubular cells in mouse kidney. Anat. Rec. 255, 316-323.

Yabuki A., Suzuki S., Matsumoto M. and Nishinakagawa H. (1999b). Morphometrical analysis of sex and strain differences in the mouse nephron. J. Vet. Med. Sci. 61, 891-896.

Yabuki A., Suzuki S., Matsumoto M. and Nishinakagawa H. (2001). Sex and strain differences in the brush border and PAS-positive granules and giant bodies of the mouse renal S3 segment cells. Exp. Anim. 50, 59-66.

Accepted July 26, 2001